Quantitative intracellular retention of delivered RNAs through optimized cell fixation and immunostaining

PRASATH PARAMASIVAM,[1] MARTIN STÖTER,[1] ELOINA CORRADI,[2] IRENE DALLA COSTA,[2,7] ANDREAS HÖIJER,[3] STEFANO BARTESAGHI,[4] ALAN SABIRSH,[3] LENNART LINDFORS,[3] MARIANNA YANEZ ARTETA,[3] PETER NORDBERG,[5] SHALINI ANDERSSON,[6] MARIE-LAURE BAUDET,[2] MARC BICKLE,[1] and MARINO ZERIAL[1]

[1]Max Planck Institute of Molecular Cell Biology and Genetics, 01307 Dresden, Germany

[2]Department CIBIO, University of Trento, Trento 38123, Italy

[3]Advanced Drug Delivery, Pharmaceutical Science R&D, AstraZeneca, 43150 Gothenburg, Sweden

[4]Bioscience Metabolism, Research and Early Development Cardiovascular, Renal and Metabolism, BioPharmaceuticals R&D, AstraZeneca, 43150 Gothenburg, Sweden

[5]Medicinal Chemistry, Research and Early Development, Cardiovascular, Renal and Metabolism (CVRM), BioPharmaceuticals R&D, AstraZeneca, 43150 Gothenburg, Sweden

[6]Oligonucleotide Discovery, Discovery Sciences R&D, AstraZeneca, 43150 Gothenburg, Sweden

ABSTRACT

Detection of nucleic acids within subcellular compartments is key to understanding their function. Determining the intracellular distribution of nucleic acids requires quantitative retention and estimation of their association with different organelles by immunofluorescence microscopy. This is particularly important for the delivery of nucleic acid therapeutics, which depends on endocytic uptake and endosomal escape. However, the current protocols fail to preserve the majority of exogenously delivered nucleic acids in the cytoplasm. To solve this problem, by monitoring Cy5-labeled mRNA delivered to primary human adipocytes via lipid nanoparticles (LNP), we optimized cell fixation, permeabilization, and immunostaining of a number of organelle markers, achieving quantitative retention of mRNA and allowing visualization of levels that escape detection using conventional procedures. The optimized protocol proved effective on exogenously delivered siRNA, miRNA, as well as endogenous miRNA. Our protocol is compatible with RNA probes of single molecule fluorescence in situ hybridization (smFISH) and molecular beacon, thus demonstrating that it is broadly applicable to study a variety of nucleic acids in cultured cells.

Keywords: nucleic acids; endosomes; fixation; immunofluorescence; smFISH; molecular beacon

INTRODUCTION

The success of nucleic acid (e.g., siRNA, mRNA, anti-sense oligonucleotides) therapeutics depends on endocytosis and subsequent escape from endosomes to reach their site of action in the cytoplasm or the nucleus (Gilleron et al. 2013; Kowalski et al. 2019). Although endocytic uptake can be relatively specific and efficient, only a tiny fraction of endocytosed nucleic acid therapeutics escapes from the endosomal lumen avoiding the ultimate degradation in lysosomes. The mechanism of nucleic acid escape from endosomes is unclear (Dowdy 2017; Setten et al. 2019). Therefore, to better understand the relationship between trafficking and escape as a prerequisite to guide the development of delivery platforms, it is important to determine the subcellular distribution of nucleic acids in different endosomal compartments. This is not a trivial task because nucleic acids can enter cells via a range of uptake mechanisms (Gilleron et al. 2013) and be transported to an endosomal network comprising several distinct endocytic compartments characterized by different transport kinetics, morphology, and biochemical composition (Schmid et al. 2014; Dowdy 2017). A prerequisite for this analysis is to obtain quantitative estimates of the colocalization of nuclei acids to endosomal compartments labeled with

[7]**Present address:** Department of Biological Sciences, University of South Carolina, Columbia, SC 29208, USA

Corresponding author: zerial@mpi-cbg.de

Article is online at http://www.rnajournal.org/cgi/doi/10.1261/rna.078895.121. Freely available online through the *RNA* Open Access option.

specific markers by high resolution microscopy and image analysis (Gilleron et al. 2013; Sahay et al. 2013). The most common approach is to use fluorescently labeled nucleic acids or detect them by single molecule fluorescence in situ hybridization (smFISH). The fluorescent nucleic acids can then be localized to endocytic compartments that are labeled by immunofluorescence staining (IFS) with specific antibodies. An alternative method is to image living cells expressing fluorescently tagged endosomal markers. However, this approach has two major drawbacks. First, cell lines expressing a panel of fluorescent endosomal markers covering the endocytic pathway are not always available. Second, it is not readily applicable to primary cells and tissues, especially human specimens. Consequently, IFS remains the simplest method for the intracellular characterization of nucleic acids. Nevertheless, the widely used method based on formaldehyde (FA) for fixation and Triton X-100 for permeabilization fails to preserve nucleic acids quantitatively, especially for siRNA, miRNAs, and mRNA (Urieli-Shoval et al. 1992; Pena et al. 2009; Klopfleisch et al. 2011; Fernández and Fuentes 2013).

Exogenous delivery of mRNA to cells has great potential for basic research but is also a major focus of nucleic acid-based therapeutics such as mRNA-based vaccines (Yanez Arteta et al. 2018; Kowalski et al. 2019). However, only a handful of studies have addressed the subcellular trafficking of the delivered mRNA (Lorenz et al. 2011; Kirschman et al. 2017). On the one hand, information on the efficiency of mRNA fixation and retention within the cytoplasm of the target cells using the standard IFS protocols is lacking. On the other hand, alternative strong fixatives, such as alcohols and glutaraldehyde, are often incompatible with antibody staining (Hopwood 1969; Farr and Nakane 1981; Hoetelmans et al. 2001). This led us to improve the methodology to retain the mRNA as well as other nucleic acids quantitatively and enable the characterization of its subcellular localization.

RESULTS

Significant loss of exogenously delivered mRNA after fixation and permeabilization

Several studies reported loss of endogenous mRNA from cells during commonly used IFS protocols (Urieli-Shoval et al. 1992; Pena et al. 2009; Klopfleisch et al. 2011; Sylwestrak et al. 2016). Exogenously delivered nucleic acids internalized in endosomal organelles must be preserved by fixation and permeabilization methods. To address this problem, we used mRNA labeled with the Cy5 fluorophore (Cy5 mRNA), formulated in lipid nanoparticles (LNP) and delivered to human primary adipocytes, as clinically relevant cell system (Yanez Arteta et al. 2018). LNP subcutaneous administration is aimed to reach the fatty layer beneath the epidermis and dermis of the skin. Primary human adipocytes are therefore the most relevant cell model to study uptake of drugs administered by this route. First, we estimated the extent of signal loss by quantifying the efficiency of mRNA fixation using a widely used formaldehyde-based protocol (3.7% for 10 min at room temperature). Although LNP Cy5 mRNA were detectable in living cells as soon as 30 min of incubation (Fig. 1A), only a very low signal was retained in fixed cells, suggesting that the fixation protocol fails to quantitatively retain mRNA in the cytoplasm. Second, we quantified the loss of mRNA upon fixation and permeabilization with detergent. For this, we incubated LNP Cy5 mRNA with adipocytes for 24 h to accumulate high levels of mRNA and maximize the signal. The cells were then fixed and permeabilized with Triton X-100. Strikingly, we estimated a loss of 83.5% ± 0.5% of Cy5 mRNA signal in cells subjected to permeabilization compared with control cells, that is, fixed and without permeabilization (Fig. 1B,C). Such a loss was not limited to mRNA, as it was also observed with siRNAs delivered via commercial transfection reagents in HeLa cells permeabilized with Triton X-100 (Fig. 1D,E). Overall, these results suggest that loss of exogenously delivered nucleic acid occurs in both fixation and permeabilization steps. These results prompted us to improve the protocol for better retention of nucleic acids in cells.

Formaldehyde concentration and incubation time are crucial to retain mRNA quantitatively

Previous studies have shown that after FA fixation, an additional fixation with 1-ethyl-3-(3-dimethylaminopropyl) carbodiimide (EDC) or disuccinimidyl suberate (DSS) can covalently fix nucleic acids in tissues (Pena et al. 2009; Sylwestrak et al. 2016). We tested these fixatives first in HeLa cells as they are easier to culture and process than primary adipocytes. To determine whether fixation with EDC and DSS is compatible with IFS of endosomal compartments, we used anti *EEA1* antibodies to label early endosomes. Although EDC and DSS fixation following FA improved the retention of Cy5 mRNA, a significant loss of signal persisted (Fig. 2A,B). Moreover, EDC treatment was incompatible with IFS as it increased the background fluorescence upon staining with *EEA1* antibodies (Fig. 2C), making colocalization-based analysis impossible. In contrast, DSS significantly reduced the *EEA1* signal in IFS. These results indicate that fixation with EDC and DSS does improve the retention of mRNA signal but is not compatible with IFS.

We therefore returned to formaldehyde-based fixation as it is a method widely applied to IFS. We tested formaldehyde at higher concentration and longer incubation times in order to improve the cross-linking of proteins and thus trap mRNA better in HeLa cells and human primary adipocytes. Our results show that higher FA concentration (7.4%) and longer incubation time (2 h) retained more signal compared with control (3.7% FA 10-min incubation)

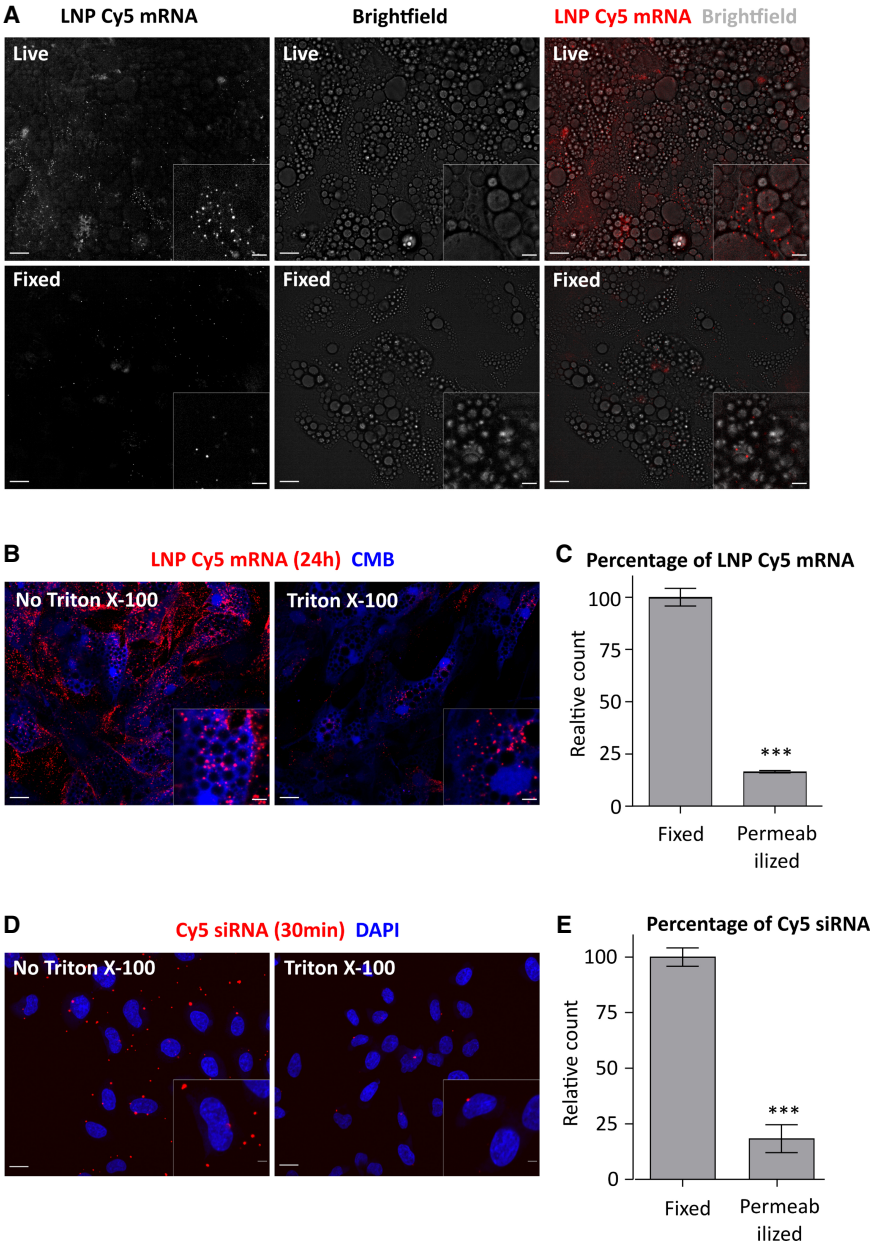

FIGURE 1. Poor Cy5 mRNA retention during cell fixation and permeabilization. (*A*) LNP Cy5 mRNA uptake (30 min) in human primary adipocytes. The amount of Cy5 mRNA signal in FA-fixed cells (3.7% for 10 min) is very low compared with living cells. The circular structures in the bright-field images are lipid droplets of adipocytes. (*B*) Representative images of cells incubated with LNP Cy5 mRNA (24 h) that were either only fixed or fixed and permeabilized with Triton X-100 (0.1%, 10 min). The dark holes in the cytoplasm correspond to lipid droplets that cannot be stained with CMB. (*C*) The quantification shows that the percentage of Cy5 mRNA object count is significantly lower in permeabilized cells compared with nonpermeabilized cells. (***) $P < 0.0001$ relative to "Fixed." All conditions were performed in triplicates, mean ± SEM. These data were taken from the experiments of Figure 3 (below). (*D*) HeLa cells incubated with the commercial transfection reagent Interferrin were either fixed or fixed and permeabilized. Representative images show loss of Cy5-siRNA in fixed cells after Triton X-100 (0.1%, 10 min) permeabilization. (*E*) Quantification of Cy5 siRNA shows 81.7% ± 6.2% loss of siRNAs in Triton X-100 permeabilized cells compared to only fixed cells. These data were taken from experiments of Figure 5B (below). $N = 3$ independent experiments. Mean ± SEM are displayed. The scale bars of full images are 20 µm, *inset* images are 5 µm.

(Fig. 2D,E). Similar results were obtained in eLa cells (Supplemental Fig. 1A). Additionally, FA with longer incubation time and higher concentration retained a comparable amount of mRNA signal to FA and DSS cofixed condition (Supplemental Fig. 1A,B). Thus, the simple modified FA fixative method is sufficient to fix mRNA better and the requirement of special mRNA fixatives is not necessary for exogenously delivered mRNA.

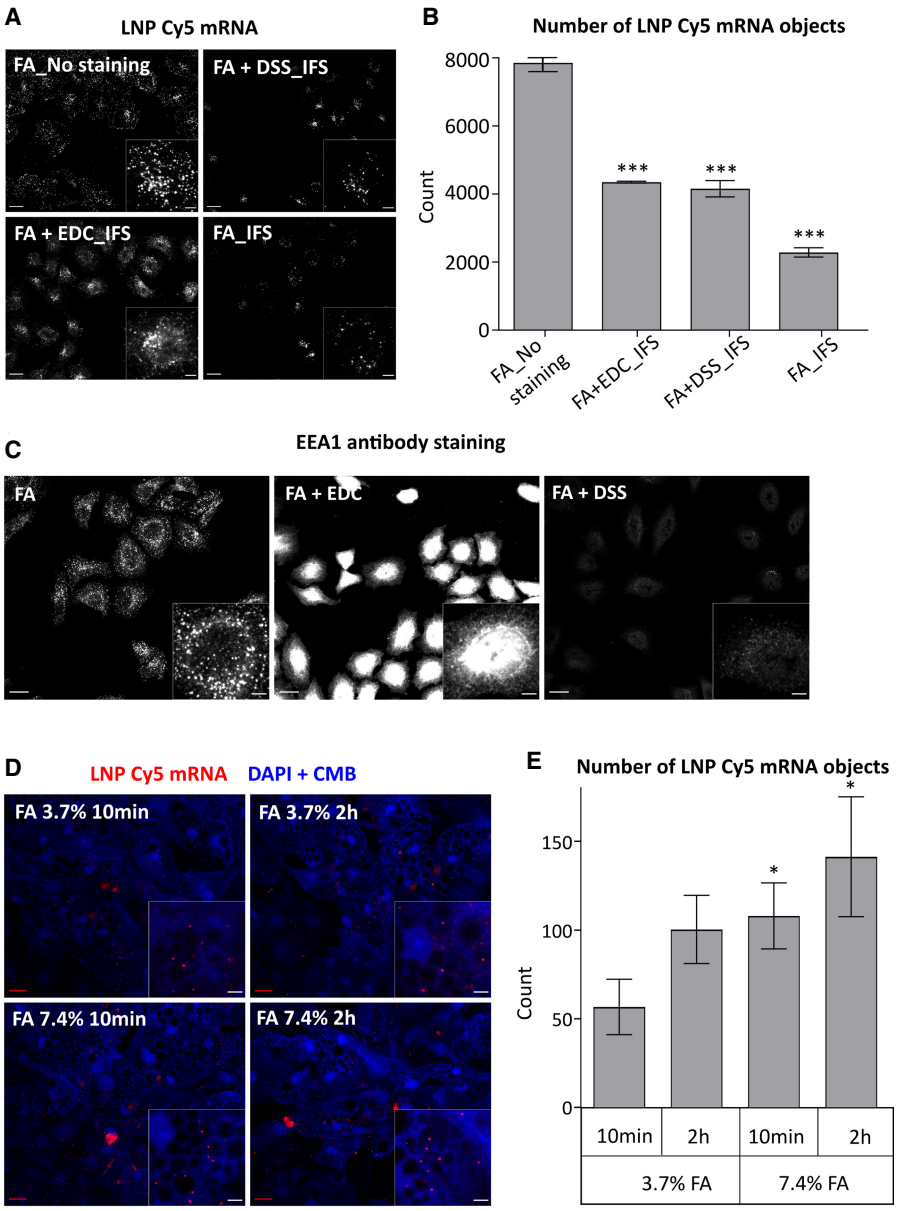

FIGURE 2. Higher FA concentration and incubation time retain more Cy5 mRNA in cells. (*A*) LNP Cy5 mRNA retention in EDC and DSS fixed HeLa cells. Cells incubated with LNP Cy5 mRNA (2 h) were either fixed with 3.7% FA (10 min) alone or fixed additionally with either EDC or DSS (2 h). The images were taken after Triton X-100 permeabilization and immunostaining with *EEA1* antibodies. (*B*) Quantification of Cy5 mRNA retention shows that after permeabilization, both EDC and DSS fixation retain more mRNA compared with cells fixed with FA alone. All conditions were performed in duplicates. (***) $P < 0.0001$ relative to "FA No staining." (*C*) Representative images of *EEA1* antibody staining. The images show artifacts upon EDC fixation and poor staining in DSS fixed conditions, indicating incompatibility with IFS. (*D*) LNP Cy5 mRNA retention after FA fixation in human primary adipocytes. Cells incubated with LNP Cy5 mRNA (30 min) were fixed with FA at concentration and incubation time as indicated. (*E*) Quantification shows improved Cy5 mRNA retention with increasing FA concentration and incubation time. (*) $P < 0.04$ relative to "FA_3.7%_10 min." All conditions were performed in triplicates. Mean ± SEM. The scale bars of full images are 20 µm and *inset* images are 5 µm.

Mild permeabilization method is crucial to retain more mRNA during IFS

A significant loss of Cy5 mRNA signal occurred during permeabilization of cells (Fig. 1B). Presumably, Triton X-100 solubilizes the endosomal membrane and causes the subsequent loss of mRNA signals that are insufficiently fixed. Saponin and Digitonin are mild detergents that interact with cholesterol and form pores on the plasma membrane but do not efficiently permeabilize the endosomal membrane (Malerød et al. 2007; Sudji et al. 2015). Such permeabilization would be sufficient for antibodies to pass

through the plasma membrane during IFS but prevent the loss of mRNA from the endosomes. We first tested previously reported conditions of Saponin and Digitonin detergents for permeabilization in HeLa cells (Villaseñor et al. 2015), in a range of concentrations below the critical micelle concentration (CMC) (Saponin CMC = 0.5g/L–0.8g/L, Digitonin CMC = 0.25–0.5 mM). Compared with nonpermeabilized cells, Digitonin retained a large proportion (93.56% ± 2.48%) of Cy5 mRNA signal in contrast to Triton X-100, which retained only a minor fraction (9.18% ± 1.08%) (Fig. 3A; Supplemental Fig. 2A). Digitonin permeabilization under this condition was also compatible with IFS as the *EEA1* antibodies signal was comparable with classical Triton X-100 permeabilization conditions (Fig. 3B; Supplemental Fig. 2B,D). Interestingly, permeabilization with Saponin reduced the Cy5 mRNA signal to 12 .5% ± 0.54%. Both Triton X-100 and Saponin showed no improvement of Cy5 mRNA signal at lower concentrations (Supplemental Fig. 2C).

Since Digitonin permeabilization did not lead to significant loss of mRNA and was compatible with IFS in HeLa cells, we proceeded to test the protocol in human primary adipocytes. Given the abundance of lipid droplets in adipocytes, we first optimized the Digitonin permeabilization step by testing various concentrations and incubation times on Cy5 mRNA retention and *EEA1* antibodies staining in comparison with Triton X-100 permeabilization. In adipocytes, 0.004% Digitonin permeabilization for 1 min

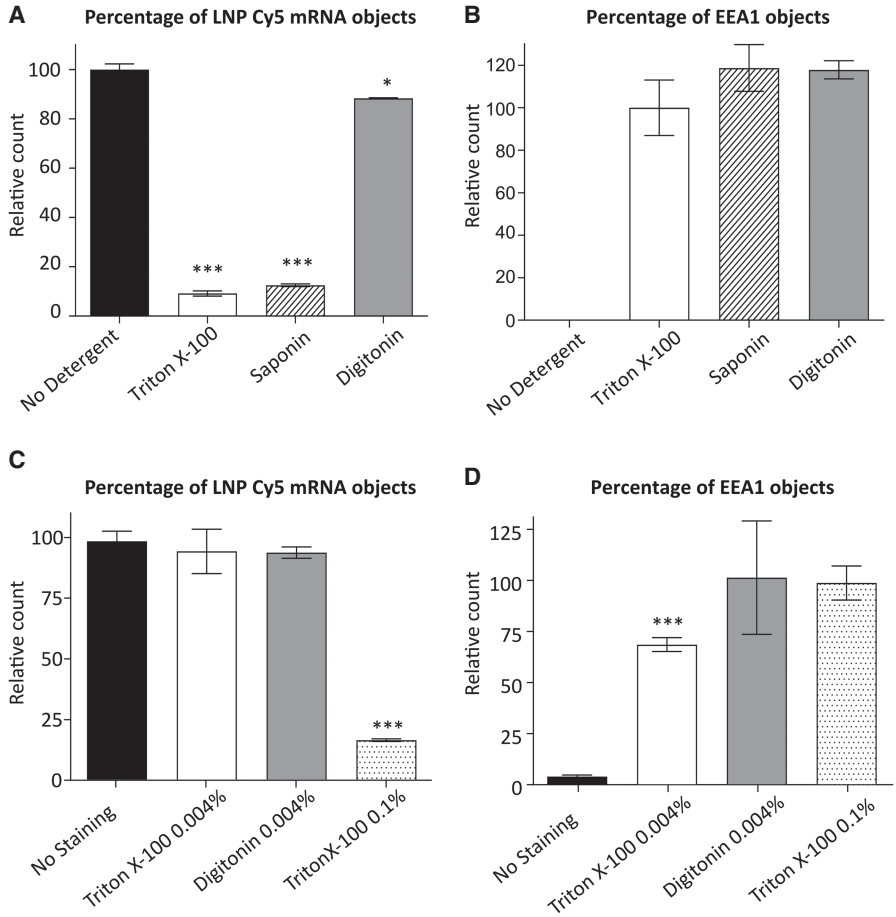

FIGURE 3. Mild cell permeabilization with Digitonin prevent loss of Cy5 mRNA. (*A*) Cy5 mRNA retention after permeabilization with detergents. HeLa cells treated with LNP Cy5 mRNA (1 h) are FA fixed (FA 3.7%, 10 min), permeabilized either with Triton X-100 (0.1%, 10 min) or Saponin (0.1%, 10 min) or Digitonin (0.001%, 1 min), and immunostained with *EEA1* antibodies. Compared with nonpermeabilized cells (no staining), both Triton X-100 and Saponin treatment show significant mRNA loss, whereas Digitonin retains mRNA signal. (*) $P = 0.053$, (***) $P < 0.0001$ relative to "No Detergent." (*B*) The graph shows that *EEA1* staining is good with all detergent permeabilization conditions (in quadruplicates). (*C*) Optimization of Digitonin permeabilization in human primary adipocytes. Cells treated with LNP Cy5 mRNA (24 h) were fixed with FA (3.7% for 10 min) and permeabilized with Digitonin or Triton X-100 at the indicated concentrations. All conditions were done in triplicates. The graph shows that Digitonin and Triton X-100 retain most mRNAs at 0.004% concentration and 1 min incubation compared with classical method (0.1% Triton X-100, 10 min). (***) $P < 0.0001$ relative to "No staining." (*D*) Quantifications of *EEA1* objects show that IFS in the Digitonin permeabilized condition is comparable with the classical method. (***) $P < 0.0008$ relative to "Triton X-100 0.1%." Nonsignificant and No staining condition *P*-values are not displayed. Mean ± SEM.

retained 95.21% ± 2.38% of mRNA signal and gave *EEA1* staining comparable with that achieved with classical 0.1% Triton X-100 10 min permeabilization (Fig. 3C,D; Supplemental Fig. 3A,B). Interestingly, the mRNA signal loss did not depend on the Digitonin incubation time (Supplemental Fig. 4A). In contrast, permeabilization with Triton X-100 yielded suboptimal results at all concentrations tested. Longer permeabilization times with Triton X-100 caused a significant loss of mRNA signal and reducing the concentration retained the mRNA signal but also reduced the *EEA1* staining (Supplemental Fig. 4A,B). When cells were permeabilized with 0.004% Triton X-100 for 1 min, 95.72% ± 9.29% of mRNA signal was retained. However, the above mentioned condition showed less IFS efficiency compared with the classical protocol (0.1% Triton X-100 for 10 min) (Fig. 3D; Supplemental Fig. 3B). Altogether, these results suggest that permeabilization with Digitonin retains most mRNA signals across various concentrations and is compatible with IFS in adipocytes.

We also found two other steps that caused major nucleic acids mRNA loss. First, in contrast to DAPI, nuclear staining with Hoechst quenched ~80% of the mRNA signal (Supplemental Fig. 5A). Second, BSA blocking caused mRNA loss presumably due to RNase contaminants (data not shown). Although usage of these reagents is not necessarily common, we recommend to avoid Hoechst or use the lowest possible concentration for fluorescence microscopy-based mRNA studies and take precautions such as including RNase inhibitor while using BSA blocking solutions.

Adaptation of improved fixation and permeabilization methods for smFISH

The optimized protocol was established using LNP delivered Cy5-mRNA. To demonstrate that the protocol is applicable to unlabeled mRNA, we tested its compatibility with smFISH, as this method is widely applied to visualize endogenous mRNA. As a prerequisite, we first verified whether the smFISH probe can efficiently detect the majority of mRNAs under our optimized protocol, by quantifying the colocalization of smFISH probe and prelabeled Cy5-mRNA. To this end, we first performed smFISH staining on LNP Cy5 mRNA deposited on glass slides. About 98.09% ± 0.48% of Cy5 mRNA were also labeled with the smFISH probe (eGFP—CAL Fluor Red 590 dye) (Supplemental Fig. 6), demonstrating that it can be used to detect the mRNA. Next, to determine whether the smFISH staining can be applied under the improved fixation and permeabilization protocol, we incubated Cy5 mRNA in adipocytes for 30 min, and fixed and permeabilized the cells as described in the previous section. We also used ethanol (EtOH) permeabilization as recommended by the smFISH probe manufacturer for comparison under our fixation condition. As shown in Figure 4B, EtOH permeabilization labeled 99.19% ± 0.02% (in HeLa cells 97.59% ± 0.25%) (Supplemental Fig. 8A) of Cy5 mRNA with the smFISH-570 probe, suggesting that 2-h fixation with 7.4% FA did not affect the smFISH (Fig. 4A,B). We also noted that the Cy5 mRNA signal was not lost after EtOH permeabilization compared with nonpermeabilization control conditions (Fig. 4C). Nonetheless, EtOH permeabilization showed insufficient labeling or produced artifacts with some antibodies tested (Supplemental Fig. 7). These results point at incompatibility between EtOH permeabilization and IFS. In contrast, Digitonin permeabilization resulted in only 81.69% ± 0.22% (in HeLa cells 74.5% ± 4.36%) (Supplemental Fig. 8B) of Cy5 mRNA labeled with the smFISH-570 probe. Overall, these results suggest that (1) higher FA concentration and longer fixation times do not affect smFISH efficiency, (2) both EtOH and Digitonin permeabilization methods retain most mRNA signal but only Digitonin is compatible with IFS, and (3) despite retaining mRNA, Digitonin permeabilization alone is insufficient for smFISH mRNA labeling.

To solve this problem, we designed a two-step permeabilization protocol for IFS and detected unlabeled mRNA using smFISH. First, after 7.4% 2-h FA fixation, we performed Digitonin permeabilization and immunostaining. Second, the cells were fixed again with classical fixation (3.7% FA for 10 min) to preserve the antibody signal after IFS. Third, we performed EtOH permeabilization and smFISH staining to label the mRNA. As shown in Figure 4D, the protocol retained about 75.69% ± 3.84% of mRNA signal and was also compatible with IFS (Supplemental Fig. 9). It is important to note that neither permeabilization with Digitonin nor with EtOH caused a significant loss of mRNA (Fig. 4C) but this occurred only upon IFS and smFISH (25% loss in adipocytes, 38% in HeLa cells) (Fig. 4D; Supplemental Fig. 8C, respectively).

Next, we tested whether our improved smFISH protocol is generally compatible with IFS of cytoplasmic organelles. For this, we tested a set of eight antibodies against various markers of organelles of the endocytic pathway, such as APPL1, Rab5, Rab11, ANKFY1, LBPA, LAMP1, CAV1, and LC3. We found that the protocol consistently retained between 75% and 95% of mRNA without compromising the quality of organelle marker staining (Supplemental Figs. 10I,J, 11A). Altogether, these results show that our modified IFS compatible protocol can be combined with smFISH and preserve a significantly higher amount of mRNA than the current protocol.

Adaptation of improved protocol for other nucleic acids

Finally, we wanted to determine whether our protocol is generally applicable to different RNAs, both endogenous and exogenously delivered. We first tested it on the retention of endogenous mRNA in HeLa cells, focusing on the Transferrin receptor (TFR) mRNA, since it is expressed in

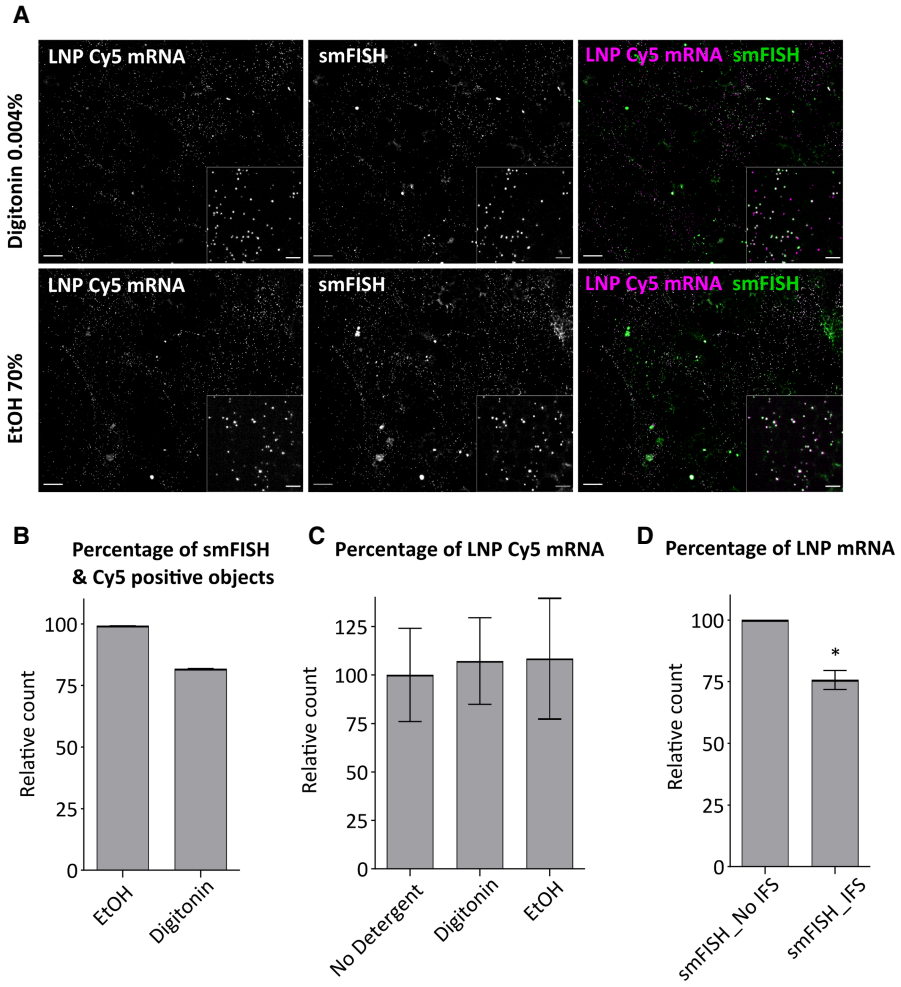

FIGURE 4. Improved fixation and permeabilization methods can be adapted for smFISH. (*A*) smFISH was performed in adipocytes incubated with LNP Cy5 mRNA after fixation (7.4% FA, 2 h) and permeabilization with ethanol or Digitonin. The images show that a subset of Cy5 mRNA is not labeled for smFISH in Digitonin permeabilized cells. All conditions were done in triplicates (*B*) The graph shows that the smFISH labeling of Cy5 mRNA is nearly 100% with ethanol, whereas a subset of Cy5 mRNA objects is not labeled in Digitonin permeabilized cells. (*C*) The graph shows retention of the Cy5 mRNA after EtOH and Digitonin permeabilization. (*D*) Adipocytes incubated with LNP unlabeled mRNA (1 h) were stained as described in the Results section. The graph illustrates that mRNA is retained after IFS. (*) $P = 0.04$ relative to smFISH_No IFS. $N = 3$ independent experiments, mean ± SEM.

a wide range of cells. We noted no TFR mRNA loss by smFISH after Triton-X 100 permeabilization compared with Digitonin permeabilized control (Supplemental Fig. 12). Therefore, the problem of lack of retention applies to exogenously delivered mRNA or siRNA but not endogenous cytoplasmic mRNA. To determine whether our method could improve the retention of exogenously delivered siRNA in HeLa cells, we tested the efficacy of the fixation and permeabilization steps. Interestingly, increased FA concentration and longer incubation time did not improve retention of siRNA (Fig. 5A). One possibility is that small nucleic acids like siRNAs (usually 22-nt base pairs) have a lower probability to be cross-linked and trapped intracellularly upon fixation than large mRNA molecules (several hundred nucleotide bases long). However, longer fixation times helped to retain more siRNAs during the permeabilization step (Fig. 5B, cf. 64.9% ± 8% siRNA retention in 10 min FA fixed cells vs. 84.7% ± 7% in 2 h FA fixed cells under Digitonin permeabilization condition). In addition, we noted that 3.7% 2-h FA fixation, sufficiently retained siRNA with good *EEA1* staining but 7.4% fixation reduced *EEA1* staining in HeLa cells (Supplemental Fig. 13). Therefore, we recommend to optimize fixative concentration in each cell model system to ensure minimum loss of siRNAs while preserving the signal by antibody staining. Moreover, similar to mRNA (Supplemental Fig. 5A), we recommend to avoid or use the lowest possible concentration of Hoechst nuclear staining as it quenched ~55% of the siRNA signal (Supplemental Fig. 5B).

Since the retention of siRNAs was improved by our protocol, we tested its effect on other forms of small nucleic acids. Endogenous microRNAs (miRNAs) can associate

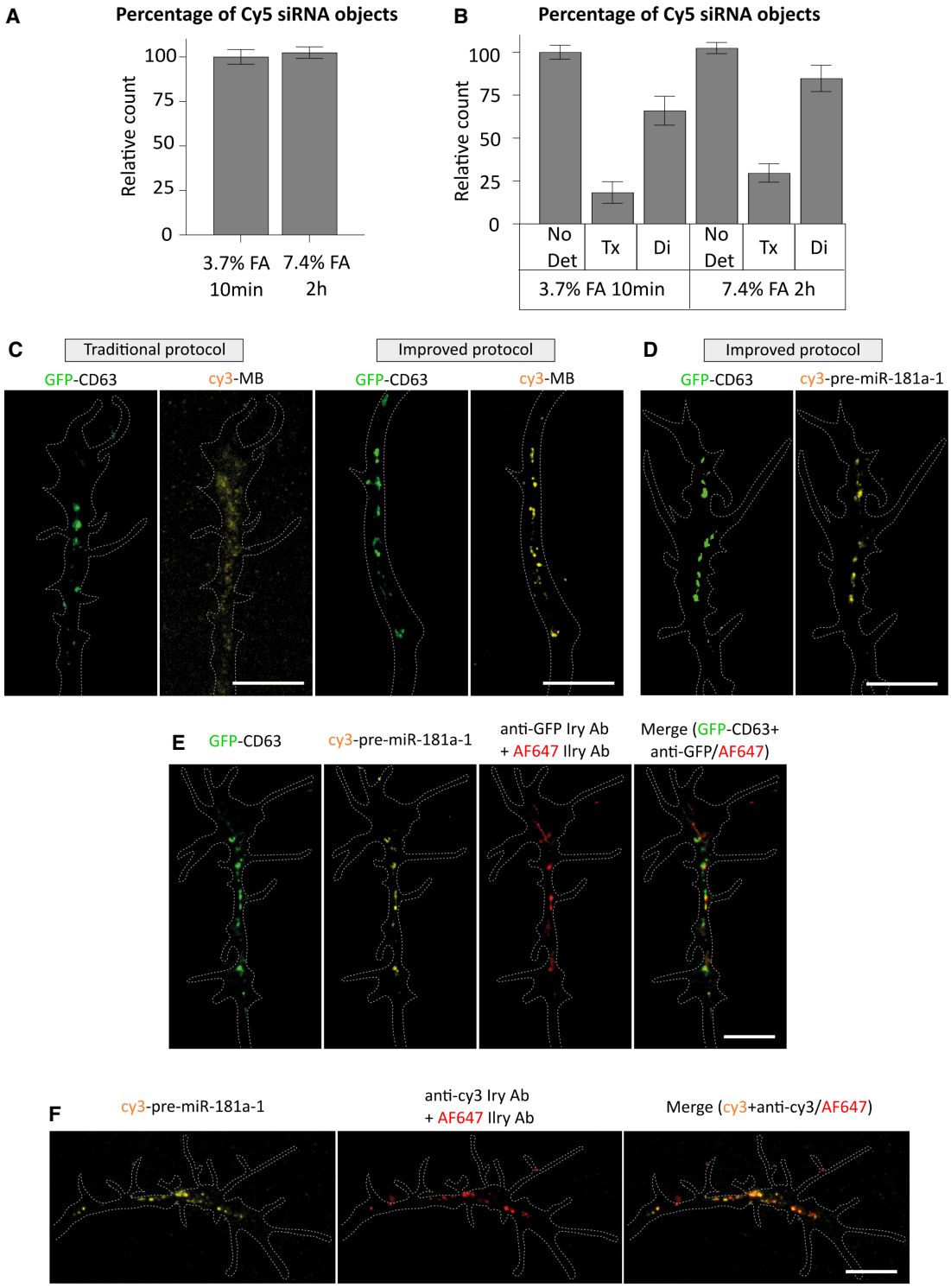

FIGURE 5. Improved intracellular retention of exogenously delivered siRNA and endogenous miRNA. (*A*) Cy5 siRNA + Interferrin incubated in HeLa cells for 30 min were fixed with FA as indicated in the graphs. In contrast to mRNA fixation data shown in Supplemental Figure 1, fixation with 7.4% FA for 2 h does not improve siRNA retention (*B*) The graph illustrates siRNA retention after 3.7% and 7.4% FA fixation (10 min) under Digitonin (0.002%, 2 min) and Triton-X (0.1%, 10 min) permeabilization. $N = 3$ independent experiments. Mean ± SEM are displayed. (*C*) Comparison of miRNA retention using traditional and improved protocol in *Xenopus laevis* organoculture. Concentrations used are as follows: 5 µM MB; 250 ng/µL cy3-pre-miR-181a-1; 0.5 µg/µL pCS2-*CD63*-eGFP (see Materials and Methods). (*D–F*) Representative images. Dashed white lines delineate axons. Compare with traditional protocol, endogenous (pre)-miRNA retention improved significantly with our optimized protocol. Fifty-four axons were analyzed in total from up to seven independent experiments. Experimental details are described in the Materials and Methods and main text. (*CD63*-eGFP) *CD63*-eGFP0expressing pCS2 plasmid, (PFA) paraformaldehyde. Scale bars, 10 µm.

with late endosomes/lysosomes (LE/Ly) and hitchhike them for intracellular transport (Gibbings et al. 2009; Lee et al. 2009; Corradi and Baudet 2020; Corradi et al. 2020). Therefore, we visualized miRNAs docked to LE/Ly by two strategies. First, we detected endogenous precursor miRNAs (pre-miRNAs) via cy3-labeled molecular beacon (MB) (Supplemental Fig. 14A; Corradi et al. 2020) and assessed its colocalization with LE/Ly marker transmembrane tetraspanin *CD63*-GFP (Pols and Klumperman 2009; Corradi et al. 2020) in elongating axons from *Xenopus laevis* whole eye explant culture (Supplemental Fig. 14B). While the standard protocol yielded a diffuse pre-miRNA-associated signal (Fig. 5C), with our optimized protocol the signal was significantly improved and appeared as discrete puncta colocalizing with *CD63*-GFP marked vesicles (Fig. 5C), consistent with previous findings in living cells (Corradi et al. 2020). Second, we investigated exogenously delivered (by electroporation) synthetic cy3-labeled pre-miRNA (Supplemental Fig. 14A,B). Again, we detected discrete puncta (Fig. 5D) as in live cells (Corradi et al. 2020), suggesting that our protocol dramatically improves the retention of both endogenous and exogenous pre-miRNAs. Finally, we tested whether our miRNA detection protocol is fully compatible with immunocytochemistry (Fig. 5E). Anti-GFP and anti-cy3 readily detected *CD63*-GFP (Fig. 5E) and cy3-labeled pre-miRNA (Fig. 5F), respectively, without altering miRNA retention.

DISCUSSION

In this study, we evaluated the retention of exogenously delivered and endogenous nucleic acids quantitatively in cells subjected to IFS using commonly used fixation and permeabilization protocols. Although numerous studies have reported the detection of RNAs by smFISH combined with immunofluorescence staining of cultured cells (Shih et al. 2011; Bayer et al. 2015; Kochan et al. 2015; Rossiello et al. 2017), the extent by which endogenous or exogenously delivered nucleic acids are preserved intracellularly has not been determined. Previous studies compared the effects of fixatives on the preservation of nucleic acids in immunohistochemical staining of tissue morphology in paraffin-embedded clinical tissue samples (Eltoum et al. 2001; Staff et al. 2013). A study reported an improvement of the hybridization step in a combined smFISH and immunofluorescence protocol by increasing the formamide concentration and incubation times, resulting in enhanced signal to noise ratio (Farack and Itzkovitz 2020). Nevertheless, to our knowledge, a systematic and quantitative assessment of nucleic acids loss from fixed and permeabilized cells by the critical steps of a protocol has not been reported yet.

Our results show that several steps, including fixative concentration, incubation times, type of detergent, Hoechst dye, BSA blocking reagent and sequence of steps can significantly influence the quantitative retention of nucleic acids as well as the quality of organelle staining. Surprisingly, although formaldehyde is a widely used and generally effective fixative agent, its application in the commonly used procedure (3.7%–4% FA and 10- to 15-min incubation) yields suboptimal nucleic acids retention. However, its efficacy can be improved by augmenting concentration and incubation times (e.g. 7.4% FA and 2-h incubation). Nonetheless, it is important to verify that the intensified macromolecular cross-linking produced by the fixative does not compromise the binding of antibodies to cellular epitopes in the immunostaining. Our results further suggest that RNA fixatives like DSS and EDC are not necessary provided other steps are optimized. Specifically, permeabilization with detergents stands out as a most critical step where the majority of nucleic acids (85%) fail to be retained in the cells. This step can be improved by optimizing detergent type, concentration and incubation times.

While our study primarily addressed the quantitative retention of exogenously delivered RNAs (siRNA, mRNA), we found that these as well as endogenous miRNA are prone to severe loss during the fixation/permeabilization procedure. This is in contrast to cytoplasmic endogenous mRNA, which is effectively retained using the standard protocols. Aldehydes, such as formaldehyde, are used to cross-link proteins by reacting with primary amines (primarily from lysine residues) to form Schiff bases that in turn can be attacked by nucleophiles (amines, thiols, and alcohols) to form intra- or intermolecular links. Formaldehyde can also react with amino groups on RNA molecules to generate interstrand–cross-linked multimers or cross-links to proteins, reducing their extractability (Feldman 1973). The efficiency of cross-linking depends on the length of the RNA and its association with, or proximity to, proteins. Both the length of mRNA molecules and their interactions with proteins in the cytoplasm render them particularly suitable to cross-linking. In contrast, a shorter RNA like miRNA proved more difficult to preserve. Additionally, nucleic acids exogenously delivered by LNP or lipid-based transfection reagents could not be efficiently cross-linked in the lumen of endosomal compartments. We can consider two additive factors to explain this behavior. First, the RNA molecules in the lumen of the endosomes are not free but tightly packaged with the lipids, none of which contains primary amines that could be used for cross-linking. Those RNA molecules that may dissociate from the lipids are unlikely to interact with specific RNA-binding proteins in that environment. Second, an additional factor is the permeability of membranes to the fixative agent. Formaldehyde is water soluble but can penetrate the plasma membrane and make it permeable. However, it may require longer incubation times to penetrate also cytoplasmic organelles without detergents. These two factors concur to make it arduous to fix RNA in the endosomal lumen under the conditions of the

standard protocols. Similarly, RNA within membrane organelles such as mitochondria may also be difficult to fix. With increasing interest in exploring the function of nucleic acids in membrane compartments (Corradi et al. 2020), we recommend devoting care to the protocol optimization to improve the efficiency of nucleic acids retention.

Surprisingly, we found that one of the commonly used nuclei staining dye, Hoechst, quenched the fluorescence signal of exogenously delivered nucleic acids. We used two different fluorophores (Cy5 labeled mRNA and Alexa 647 labeled siRNA) in our imaging experiments, suggesting that the loss of nucleic acid fluorescence signal in cells upon incubation with Hoechst is not a peculiarity of a single fluorophore. We did not observe eGFP protein fluorescence loss in the presence of Hoechst (data not shown). Our results raise the possibility that Hoechst may interfere with the microscopy imaging of RNA in general.

In conclusion, we outlined an improved fixation and IFS methodology that can retain quantitative amounts of exogenously delivered mRNA, siRNA and miRNA, as well as endogenous miRNA in the cell cytoplasm. This methodology is especially critical when the intracellular levels of RNA are low. Our optimized protocol was applied .to adipocytes, HeLa cells and axons from *Xenopus laevis* whole-eye explant culture, suggesting that it is generally applicable with minor modifications depending on the specific cell type. Our study can guide and offer appropriate solutions to researchers who study nucleic acids in various cell model systems to focus on critical steps, save time, resources as well as enable studies that were previously not feasible due to significant nucleic acid loss (similar to miRNA detection in endosome trafficking in axons). Since our methodology is compatible with probes of smFISH and molecular beacon, we hope it will be broadly applied to fluorescence-based quantification studies of various forms of exogenously delivered and endogenous nucleic acids.

MATERIALS AND METHODS

Cell culture

HeLa cells were cultured in DMEM media complemented with 10% FBS Superior (Merck S0615) and 50 µg/mL gentamicin (Gibco G1397) at 37°C with 5% CO_2. The day before a transfection 3000 HeLa cells in a 50 µL/well were seeded in 384-well plates using the drop dispenser (Multidrop, Thermo Fisher Scientific).

Human adipose stem cells (hASCs) from human subcutaneous white adipose tissue (WAT) were provided by AstraZeneca. hASCs were collected from patients undergoing elective surgery at Sahlgrenska University Hospital in Gothenburg, Sweden. All study subjects received written and oral information before giving written informed consent for the use of the tissue. The studies were approved by The Regional Ethical Review Board in Gothenburg, Sweden. All procedures performed in studies involving human participants were in accordance with the ethical standards of the institutional and national research committee and with the 1964 Helsinki Declaration and its later amendments or comparable ethical standards. All subjects complied with ethical regulations. We adapted protocol from AstraZeneca (AZ) to differentiate hASCs to mature white-like adipocytes in 384-well format. Briefly, cryopreserved human adipose stem cells were resuspended in EGM-2 medium and centrifuged at 200*g* for 5 min. EGM-2 medium was prepared according to the manufacturer's protocol with EBM-2 medium supplemented with 5% FBS, all provided supplements, except hydrocortisone and GA-1000 (Lonza 3202, EGM-2 MV BulletKit [CC-3156 and CC-41472]). Cells were counted with a CASY cell counter (Schärfe System) and 4000 cells per well were seeded in 50 µL of EGM-2 medium containing 50 U/mL penicillin and 50 µg/mL streptomycin (P/S) (Gibco 15140-122) into 384-well plates (Greiner Bio-One, 781092) using the drop dispenser Multidrop. The cells were incubated for 3–4 d at 37°C and 5% CO_2. For adipocyte differentiation, 90% confluent cells were incubated for 1 wk with Basal Medium (Zenbio BM-1) supplemented with 3% FBS Superior, 1 µM dexamethasone (Sigma Aldrich), 500 µM 3-isobutyl-1-methyxanthine (Sigma Aldrich), 1 µM pioglitazone (provided by AZ), P/S and 100 nM insulin (Actrapid Novo Nordisk, provided by AZ). Medium was replaced with BM-1 medium supplemented with 3% FBS Superior, 1 µM dexamethasone, P/S, and 100 nM insulin and cells were incubated for another 5 d. hASCs were tested and found free of mycoplasma.

Chemicals

Formaldehyde (Merck), Triton X-100 (SERVA Electrophoresis GmbH), Digitonin (Sigma Aldrich) and Saponin (Sigma Aldrich), l-ethyl-3-(3-dimethylaminopropyl) carbodiimide (EDC) (Pierce 22980), Disuccinimidyl suberate (DSS) (Pierce 21555), FBS Superior (Merck S0615), dexamethasone (Sigma Aldrich, D2915), 3-isobutyl-1-methyxanthine (Sigma Aldrich I5879), Insulin (Actrapid Novo Nordisk) and Pioglitazone (AZ10080838) were provided by AstraZeneca. Penicillin and streptomycin (Gibco 15140-122). LNPs were prepared with ((2-(dimethylamino)ethyl)azanediyl)bis (hexane-6,1-diyl)bis(2-hexyldecanoate) (AstraZeneca), cholesterol (Sigma Aldrich), 1,2-distearoyl-sn-glycero-3-phosphocholine (DSPC; CordenPharma), dn 1,2-dimyristoyl-sn-glycero-3-phosphoethanolamine-N [methoxy (polyethyleneglycol)-2000] (DMPE-PEG2000; NOF Corporation) and contained CleanCap enhanced green fluorescent protein (eGFP) mRNA (5-methoxyuridine) (TriLink Biotechnologies L-7201) and/or Clean Cap-Cyanine5 (Cy5) enhanced green fluorescent protein mRNA (5-methoxyuridine) (TriLink Biotechnologies L-7701).

LNP preparation and characterization

LNP were formulated by a bottom-up approach (Zhigaltsev et al. 2012) using a NanoAssemblr microfluidic apparatus (Precision NanoSystems Inc.). Prior to mixing, the lipids were dissolved in ethanol and mixed in the appropriate ratios while mRNA was diluted in RNase free 50 mM citrate buffer (pH 3.0; Teknova). The aqueous and ethanol solutions were mixed in a 3:1 volume ratio at a mixing rate of 12 mL/min to obtain LNP with a mRNA:lipid weight ratio of 10:1. Finally, they were dialyzed overnight using Slide-A-Lyzer G2 dialysis cassettes with a molecular weight cutoff

of 10 K (Thermo Fisher Scientific). The size was determined by DLS measurements using a Zetasizer Nano ZS (Malvern Instruments Ltd.) The encapsulation and concentration of mRNA were determined using the Ribo-Green assay.

LNP mRNA transfection

HeLa cells were transfected in the presence of 10% FBS Superior. Transfection for mature human white-like adipocytes was performed in the presence of fresh BM-1 medium supplemented with 1% human serum (Sigma H4522). Both HeLa cells and mature human white-like adipocytes were transfected with LNPs at a final mRNA concentration of 1.25 µg/mL. LNP incubation times varied from 30 min to 24 h and is given for each experiment in the figure legends.

siRNA transfection

Alexa 647-labeled siRNAs were complexed with Interferrin (PolyPlus) for 10 min in OptiMEM (siRNA final concentration = 10nM, Interferrin final volume/well/50 µL in 384-well plate format = 0.1µL), added to HeLa cells in 10% FBS and incubated for 30 min before washing and fixation. Fluorophore labeled siRNAs were ordered from Sigma Aldrich and sequences used are as follows. Sense strand: Alexa Fluor 647—5′-ACAUGAAGC AGCACGACUUdTdT-3′; antisense strand: 5′-AAGUCGUGCUG CUUCAUGUdTdT-3′.

Cell fixation

After LNP incubation, the cells were washed with PBS using the plate washer Power Washer 384 (PW384, Tecan). The wash protocol consists of eight cycles of dispensing 100 µL of PBS followed by aspiration until a 20-µL volume remained in the well, except in the final aspiration cycle, which left a 25-µL volume. The same program was used for all washing steps specified in this article unless otherwise mentioned. The cells were then fixed with formaldehyde by adding 25 µL (2× concentrated solution prepared in nuclease-free PBS) on top of the 25 µL of remaining PBS per well using the drop dispenser (WellMate, Thermo Fisher Scientific) and washed three times with PBS using Power Washer 384. The percentage of formaldehyde (FA) and incubation time for experiments are given in figure legends. After FA fixation, an additional fixation with EDC for 2 h was performed when required following previously reported procedure (Pena et al. 2009). Briefly, the FA cells were washed with PBS, the liquid removed using an eight needle vacuum aspirator and incubated with 0.2% glycine (90 µL per well) to quench remaining FA. The cells were incubated with methyl imidazole buffer two times each for 10 min. The solution was replaced with freshly prepared EDC (20 µL/well, 0.16 M EDC in 0.13 M methyl imidazole buffer) and cells were incubated for 2 h at room temperature. Following EDC fixation, the cells were washed with PBS and incubated with 0.2% glycine as described above for 5 min and washed three times with PBS. DSS fixation was performed for 2 h at room temperature following slightly modified manufacturer's protocol (Thermo Fisher Scientific MAN0011240). The FA fixed cells were washed with PBS and replaced with 25 µL of 0.5 mM DSS dissolved in DMSO. After 2 h, the cells were washed three times with PBS. In some experiments, cofixation of FA and DSS was used instead of sequential fixation for fast processing. Briefly, a stock solution was prepared by adding FA directly from 37% to a DSS DMSO solution. This stock solution was then directly added (25 µL of 2× concentrated solution added on top of 25 µL of remaining PBS per well) to cells to reach the final concentration. The fixed cells were then washed, and the nuclei stained for imaging.

Immunofluorescence staining

Cells were permeabilized either with Triton X-100, Saponin, or Digitonin. The permeabilization conditions are described in the figure legends. All detergents were added to cells using the liquid handling robot Biomek FX (Beckman Coulter) equipped with a 384 disposable tip head. After permeabilization, the cells were washed with 3× PBS and incubated with 3% BSA PBS blocking solution (added 25 µL of 2× solution on top of 25-µL remaining volume/well) for 30 min. The blocking solution was aspirated using Power Washer 384 leaving a 12.5-µL volume per well. Primary antibodies were incubated (in 3% BSA PBS solution, added 12.5 µL on top of 12.5 µL of remaining PBS per well) for either 1 h (HeLa cells) or 2 h (human primary white-like adipocytes) to label endosomes. The cells were then washed with PBS, the liquid aspirated leaving 12.5 µL followed by incubation with secondary antibodies (prepared in 6% BSA PBS solution, 12.5 µL of solution added on top of 12.5 µL of remaining PBS per well to reach 3% final BSA concentration and required antibody dilution) for 1 h. All blocking and antibody solutions were added using the liquid handling robot Fluent, and washing steps were performed with Power Washer 384 (PW384; Tecan). After immunostaining, the cells were incubated with 1 µg/mL DAPI and 0.25 µg/mL CMB to stain the cell nuclei and the cytoplasm, respectively. All antibodies used in adipocytes and HeLa cells are listed in Supplemental Table 1.

Single-molecule fluorescent in situ hybridization (smFISH) and immunofluorescence staining

smFISH was performed using reagents, including eGFP-CAL Fluor Red 590 dye probe and Transferrin receptor endogenous mRNA Alexa Fluor 647 probe, from Stellaris. The protocol was compiled and modified from different manuals available from the manufacturer's website (https://www.biosearchtech.com/support/resources/stellaris-protocols). Buffers were prepared according to the manufacturer, and volumes adapted to the 384-well plate format. In brief, after LNP incubation, the cells were fixed for 2 h with 7.4% final concentration of formaldehyde (25 µL of 2× solution added on top of 25 µL of remaining PBS per well) at room temperature. After washing with PBS, the supernatant was removed manually with an eight-needle aspirator and 40 µL of 70% ethanol was added for 1 h at 4°C. Under Digitonin permeabilization conditions, 0.004% Digitonin (25 µL of 2× solution added on top of 25 µL of remaining PBS per well) was added for 2 min (adipocytes) or 0.001% for 1 min (HeLa cells). Note: Digitonin was first purified according to manufacturers' protocol (https://www.sigmaaldrich.com/content/dam/sigma-aldrich/docs/Sigma/Product_Information_Sheet/d5628pis.pdf). Since Digitonin is a natural extract subject to batch variation, we recommend either purifying a large batch sufficient for long-term use or

optimizing the concentration for every single batch. After washing the cells with PBS using the plate washer PW384, cells were incubated in Wash Buffer A (40 µL/well) for 2–5 min. After removal of the supernatant, the probe was added to the cells diluted in 1:100 hybridization buffer (12.5 µL/well, smFISH probe final concentration of 100 nM) for ~16 h at 37°C. The supernatant was removed and replaced twice with 40 µL Wash Buffer A for an incubation times of 30 min at 37°C Finally, Wash Buffer A was replaced with Wash Buffer B for 2–5 min. Finally, Wash Buffer A was removed and 1 µg/mL DAPI and 0.25 µg/mL CMB in RNase-free PBS were used to stain the cell nuclei and the cytoplasm as described below. For sequential IFS and smFISH protocol, the fixed cells were first permeabilized with Digitonin, stained following the IFS protocol and fixed a second time with 3.7% FA for 10 min at room temperature. Then the smFISH staining protocol was proceeded as described above with a second permeabilization with ethanol. All antibodies used in this study are given in Supplemental Table 1.

Fluorescence imaging and quantification

Where indicated, fixed cells were stained with 1 µg/mL 4′,6-diamidino-2-phenylindole (DAPI) and/or 0.5 µg/mL Cell Mask Blue (CMB). All imaging was performed on an automated spinning disc confocal microscope (Yokogawa CV7000) using a 60× 1.2 NA objective. Live cell imaging was done at 37°C, 5% CO_2, and humidified atmosphere. DAPI and CMB were acquired with a laser excitation at 405 nm and an emission band pass filter BP445/45, GFP and Alexa 488 with a 488-nm laser and BP525/50 filter, CAL Fluor Red 590 with a 561-nm laser and BP600/37 filter, Cy5 and Alexa 647 with a 640-nm laser and a BP676/29 filter, and a bright-field using a halogen lamp. In most cases, six images were acquired per well and each condition was done in triplicate wells. An average of 522 cells ± 3.5 were analyzed per condition in the experiments with adipocytes and 582 cells ± 3.49 in the experiments with HeLa cells.

Image analysis was performed in custom designed software, MotionTracking (Collinet et al. 2010). Images were first corrected for illumination, chromatic aberration and physical shift using multicolor beads. All fluorescent objects in corrected images were then segmented, and their number and intensity per image mask area were calculated.

Image analysis was also done using Fiji (Schindelin et al. 2012) and CellProfiler (Carpenter et al. 2006) software. In brief, corrected images were preprocessed for segmentation in Fiji, LNP spots and nuclei were segmented and quantified in CellProfiler. Spot measurements for shape and intensities, as well as for spatial intensity distributions, were loaded into KNIME data analysis software (Berthold et al. 2008). Detected objects from autofluorescence were removed using a Random Forest classification algorithm. Data were visualized in KNIME and with customized R scripts.

Xenopus laevis

Xenopus laevis embryos were obtained from in vitro fertilization, raised at 14°C–22°C in 0.1× Marc's Modified Ringer's (MMR; pH 7.5) and staged according to the table of Nieuwkoop and Faber (1994). All animal experiments were approved by the Italian Minister of Health with the authorization numbers 1159/2016-PR and 546/2017-PR according to article 31 of D.lgs. 26/2014.

Xenopus laevis eye electroporation

Stage 26 embryos were anesthetized in 0.3 mg/mL Tricaine methanesulfonate (MS222) (Sigma) in 1× MBS. The retinal primordium was injected with 0.5 µg/µL pCS2-*CD63*-GFP plasmid and 5 µM Molecular Beacon (MB) or 250 ng/µL pre-miRNA-181a-1, followed by electric pulses of 50-msec duration at 1000-msec intervals, delivered at 18 V.

Xenopus laevis organoculture

Cultures were performed as previously described (Bellon et al. 2017). Briefly, glass-bottom dishes (MatTek) were first coated with 10 µg/mL poly-L-lysine (Sigma) for 3 h at 20°C and then with 10 µg/mL Laminin (Sigma) for 1 h at 20°C. Eyes were dissected from stage 27 anesthetized embryos and cultured for 40 h at 20°C in 60% L-15 and 1% antibiotic–antimycotic (Thermo Fisher Scientific).

Fixation and IFS in *Xenopus laevis* organoculture

Conventional protocol fixation and IFS were performed as follows. Organocultures were fixed in 2% PFA (Thermo Fisher Scientific), 7.5% sucrose (ACS reagent) for 30 min, and the fixed samples were permeabilized with 0.1% Triton X-100 (Fisher Chemical) in PBS 1× for 10 min.

For improved fixation and IFS, organocultures were fixed in 3.7% PFA (Thermo Fisher Scientific), 7.5% sucrose (ACS reagent) for 2 h, washed three times with PBS 1× (5 min per wash), incubated in EtOH 70% (Sigma) for 1 h at room temperature, and washed three times again in PBS 1×. Cultures were permeabilized in 0.004% ethanol-purified Digitonin (Sigma) for 2 min and blocked in filtered RNase-free 3% BSA for 30 min. Rabbit polyclonal anti-GFP (1:500; Thermo Fisher Scientific A-11122) or mouse anti-cy3 (1:500; Santa Cruz Biotechnology sc-166894) were used. Primary antibodies were diluted in 3% BSA and incubated at room temperature for 2 h. Secondary antibodies Alexa Fluor AF-647 anti-rabbit (1:1000; Thermo Fisher Scientific A-21246) or anti-mouse (1:1000; Thermo Fisher Scientific A-21237) were incubated for 45 min at room temperature. Cultures were washed thrice with 1× PBS and images were acquired without mounting as described below.

Retinal ganglion cells (RGC) axons acquisition

A Nikon Eclipse Ti2 inverted microscope equipped with Lumecor Spectra X LED light source and sCMOS camera (AndorZyla 4.2 Mp) was used with a Plan Apochromatic 60×/1.4 oil objective. The acquisition mode was set to 12-bit and Gain4 (GFP and cy3 channel) and Gain 1 (cy5 channel) with a "Readout Rate" of 540 MHz and no binning. Exposure time and light intensity were kept invariant for the same batch of analysis. Representative images were adjusted for brightness and contrast.

Pre-miRNA in vitro synthesis and labeling

Pre-miR-181a-1 DNA template was obtained by two oligos (sequence below) after annealing and elongation at 12°C using 25U T4 DNA polymerase (NEB). The DNA template was purified with NucleoSpin PCR Clean-up kit (Macherey-Nagel). Pre-miR-181a-1 in vitro synthesis was performed using the T7 MEGAshortscript kit (Ambion) from 1 µg purified DNA and following manufacturer's instructions, including template removal by DNase TURBO digestion. An amount of 5 µg of pre-miR-181a-1 was labeled with cy3 using the Nucleic Acid Labeling kit (Mirus) following the manufacturer's instructions.

Pre-miR-181a-1_T7_Fw: 5′-TAATACGACTCACTATAGAACATTCAACGCTGTCGGTGAGTTTGGTATCTAAAGGC-3′

Pre-miR-181a-1_Rv: 5′-TGTACAGTCAACGATCGATGGTTTGCCTTTAGATACCAAACTCACCG-3′

Oligonucleotides and plasmid

cy3-BHQ2 pre-miR-181a-1 molecular beacon (Eurogentec): 5′-CAUUGC**C**UUUA**G**AUACCAAUG-3′, 2′-O-methyl ribose backbone and 2 LNA nucleotides (bold) (Corradi et al. 2020). Plasmid, pCS2-*CD63*-eGFP (Corradi et al. 2020).

SUPPLEMENTAL MATERIAL

Supplemental material is available for this article.

COMPETING INTEREST STATEMENT

A.H., S.B., A.S., L.L., M.Y.A., P.N., and S.A. are employed by AstraZeneca R&D Gothenburg.

ACKNOWLEDGMENTS

We thank Dr. Yannis Kalaidzidis and Dr. Christina Nadler for helpful discussions and suggestions. We also thank the following Services and Facilities of the Max Planck Institute of Molecular Cell Biology and Genetics for their support: Light Microscopy Facility (LMF) and the High-Throughput Technology Development Studio (HT-TDS) Facility. We thank the Center for Information Services and High Performance Computing (ZIH) of the TU Dresden for the generous provision of computing power. This work was financially supported by the Max Planck Society (MPG) and Astra Zeneca. E.C., I.D.C., and M.-L.B. also thank Marie Curie Career Integration (618969 GUIDANCE-miR), G. Armenise-Harvard Foundation, MIUR SIR (RBSI144NZ4), and MIUR PRIN 2017 (2017A9MK4R) grants (to M.-L.B.) for funding this research.

Author contributions: M.Z., P.P., M.S., and M.B. designed the experiments. M.Y.A. formulated LNPs. P.P. and M.S. performed experiments in cells. M.S. performed automated image acquisitions. E.C., I.D.C., and M.-L.B. designed, analyzed, and interpreted experiments in miRNAs. E.C. and M.-L.B. wrote the miRNA part of the manuscript. A.H., S.B., A.S., L.L., P.N., and S.A. commented on results and interpretations. M.Z. and P.P. wrote the manuscript with edits by M.S., M.B., and M.Y.A.

Received July 6, 2021; accepted December 12, 2021.

REFERENCES

Bayer LV, Batish M, Formel SK, Bratu DP. 2015. Single-molecule RNA in situ hybridization (smFISH) and immunofluorescence (IF) in the *Drosophila* egg chamber. *Methods Mol Biol* **1328:** 125–136. doi:10.1007/978-1-4939-2851-4_9

Bellon A, Iyer A, Bridi S, Lee FCY, Ovando-Vázquez C, Corradi E, Longhi S, Roccuzzo M, Strohbuecker S, Naik S, et al. 2017. miR-182 regulates Slit2-mediated axon guidance by modulating the local translation of a specific mRNA. *Cell Rep* **18:** 1171–1186. doi:10.1016/j.celrep.2016.12.093

Berthold MR, Cebron N, Dill F, Gabriel TR, Kötter T, Meinl T, Ohl P, Sieb C, Thiel K, Wiswedel B. 2008. *KNIME: the Konstanz information miner*. Springer, Berlin, Heidelberg. http://www.knime.com.

Carpenter AE, Jones TR, Lamprecht MR, Clarke C, Kang IH, Friman O, Guertin DA, Chang JH, Lindquist RA, Moffat J, et al. 2006. CellProfiler: image analysis software for identifying and quantifying cell phenotypes. *Genome Biol* **7:** R100. doi:10.1186/gb-2006-7-10-r100

Collinet C, Stöter M, Bradshaw CR, Samusik N, Rink JC, Kenski D, Habermann B, Buchholz F, Henschel R, Mueller MS, et al. 2010. Systems survey of endocytosis by multiparametric image analysis. *Nature* **464:** 243–249. doi:10.1038/nature08779

Corradi E, Baudet ML. 2020. In the right place at the right time: miRNAs as key regulators in developing axons. *Int J Mol Sci* **21:** 22. doi:10.3390/ijms21228726

Corradi E, Dalla Costa I, Gavoci A, Iyer A, Roccuzzo M, Otto TA, Oliani E, Bridi S, Strohbuecker S, Santos-Rodriguez G, et al. 2020. Axonal precursor miRNAs hitchhike on endosomes and locally regulate the development of neural circuits. *EMBO J* **39:** e102513. doi:10.15252/embj.2019102513

Dowdy SF. 2017. Overcoming cellular barriers for RNA therapeutics. *Nat Biotechnol* **35:** 222–229. doi:10.1038/nbt.3802

Eltoum I, Fredenburgh J, Grizzle WE. 2001. Advanced concepts in fixation: 1. Effects of fixation on immunohistochemistry, reversibility of fixation and recovery of proteins, nucleic acids, and other molecules from fixed and processed tissues. 2. Developmental methods of fixation. *J Histotechnol* **24:** 201–210. doi:10.1179/his.2001.24.3.201

Farack L, Itzkovitz S. 2020. Protocol for single-molecule fluorescence in situ hybridization for intact pancreatic tissue. *STAR Protoc* **1:** 100007. doi:10.1016/j.xpro.2019.100007

Farr AG, Nakane PK. 1981. Immunohistochemistry with enzyme labeled antibodies: a brief review. *J Immunol Methods* **47:** 129–144. doi:10.1016/0022-1759(81)90114-9

Feldman MY. 1973. Reactions of nucleic acids and nucleoproteins with formaldehyde. *Prog Nucleic Acid Res Mol Biol* **13:** 1–49. doi:10.1016/S0079-6603(08)60099-9

Fernández J, Fuentes R. 2013. Fixation/permeabilization: new alternative procedure for immunofluorescence and mRNA in situ hybridization of vertebrate and invertebrate embryos. *Dev Dyn* **242:** 503–517. doi:10.1002/dvdy.23943

Gibbings DJ, Ciaudo C, Erhardt M, Voinnet O. 2009. Multivesicular bodies associate with components of miRNA effector complexes and modulate miRNA activity. *Nat Cell Biol* **11:** 1143–1149. doi:10.1038/ncb1929

Gilleron J, Querbes W, Zeigerer A, Borodovsky A, Marsico G, Schubert U, Manygoats K, Seifert S, Andree C, Stoter M, et al. 2013. Image-based analysis of lipid nanoparticle-mediated siRNA delivery, intracellular trafficking and endosomal escape. *Nat Biotechnol* **31:** 638–646. doi:10.1038/nbt.2612

Hoetelmans RWM, Prins FA, Velde IC-t, van der Meer J, van de Velde CJH, van Dierendonck JH. 2001. Effects of acetone, methanol, or paraformaldehyde on cellular structure, visualized by reflection contrast microscopy and transmission and scanning

electron microscopy. *Appl Immunohistochem Mol Morphol* **9:** 346–351. doi:10.1097/00129039-200112000-00010

Hopwood D. 1969. Fixatives and fixation: a review. *Histochem J* **1:** 323–360. doi:10.1007/BF01003278

Kirschman JL, Bhosle S, Vanover D, Blanchard EL, Loomis KH, Zurla C, Murray K, Lam BC, Santangelo PJ. 2017. Characterizing exogenous mRNA delivery, trafficking, cytoplasmic release and RNA–protein correlations at the level of single cells. *Nucleic Acids Res* **45:** e113. doi:10.1093/nar/gkx290

Klopfleisch R, Weiss AT, Gruber AD. 2011. Excavation of a buried treasure–DNA, mRNA, miRNA and protein analysis in formalin fixed, paraffin embedded tissues. *Histol Histopathol* **26:** 797–810.

Kochan J, Wawro M, Kasza A. 2015. Simultaneous detection of mRNA and protein in single cells using immunofluorescence-combined single-molecule RNA FISH. *BioTechniques* **59:** 209–221. doi:10.2144/000114340

Kowalski PS, Rudra A, Miao L, Anderson DG. 2019. Delivering the messenger: advances in technologies for therapeutic mRNA delivery. *Mol Ther* **27:** 710–728. doi:10.1016/j.ymthe.2019.02.012

Lee YS, Pressman S, Andress AP, Kim K, White JL, Cassidy JJ, Li X, Lubell K, Lim DH, Cho IS, et al. 2009. Silencing by small RNAs is linked to endosomal trafficking. *Nat Cell Biol* **11:** 1150–1156. doi:10.1038/ncb1930

Lorenz C, Fotin-Mleczek M, Roth G, Becker C, Dam TC, Verdurmen WPR, Brock R, Probst J, Schlake T. 2011. Protein expression from exogenous mRNA: uptake by receptor-mediated endocytosis and trafficking via the lysosomal pathway. *RNA Biol* **8:** 627–636. doi:10.4161/rna.8.4.15394

Malerød L, Stuffers S, Brech A, Stenmark H. 2007. Vps22/EAP30 in ESCRT-II mediates endosomal sorting of growth factor and chemokine receptors destined for lysosomal degradation. *Traffic* **8:** 1617–1629. doi:10.1111/j.1600-0854.2007.00630.x

Nieuwkoop PD, Faber J. 1994. *Normal table of* Xenopus laevis *(Daudin)*. Garland, New York/London.

Pena JTG, Sohn-Lee C, Rouhanifard SH, Ludwig J, Hafner M, Mihailovic A, Lim C, Holoch D, Berninger P, Zavolan M, et al. 2009. miRNA in situ hybridization in formaldehyde and EDC-fixed tissues. *Nat Methods* **6:** 139–141. doi:10.1038/nmeth.1294

Pols MS, Klumperman J. 2009. Trafficking and function of the tetraspanin CD63. *Exp Cell Res* **315:** 1584–1592. doi:10.1016/j.yexcr.2008.09.020

Rossiello F, Aguado J, Sepe S, Iannelli F, Nguyen Q, Pitchiaya S, Carninci P, d'Adda di Fagagna F. 2017. DNA damage response inhibition at dysfunctional telomeres by modulation of telomeric DNA damage response RNAs. *Nat Commun* **8:** 13980. doi:10.1038/ncomms13980

Sahay G, Querbes W, Alabi C, Eltoukhy A, Sarkar S, Zurenko C, Karagiannis E, Love K, Chen D, Zoncu R, et al. 2013. Efficiency of siRNA delivery by lipid nanoparticles is limited by endocytic recycling. *Nat Biotechnol* **31:** 653–658. doi:10.1038/nbt.2614

Schindelin J, Arganda-Carreras I, Frise E, Kaynig V, Longair M, Pietzsch T, Preibisch S, Rueden C, Saalfeld S, Schmid B, et al. 2012. Fiji: an open-source platform for biological-image analysis. *Nat Methods* **9:** 676–682. doi:10.1038/nmeth.2019

Schmid SL, Sorkin A, Zerial M. 2014. Endocytosis: past, present, and future. *Cold Spring Harb Perspect Biol* **6:** a022509. doi:10.1101/cshperspect.a022509

Setten RL, Rossi JJ, Han S-p. 2019. The current state and future directions of RNAi-based therapeutics. *Nat Rev Drug Discov* **18:** 421–446. doi:10.1038/s41573-019-0017-4

Shih JD, Waks Z, Kedersha N, Silver PA. 2011. Visualization of single mRNAs reveals temporal association of proteins with microRNA-regulated mRNA. *Nucleic Acids Res* **39:** 7740–7749. doi:10.1093/nar/gkr456

Staff S, Kujala P, Karhu R, Rökman A, Ilvesaro J, Kares S, Isola J. 2013. Preservation of nucleic acids and tissue morphology in paraffin-embedded clinical samples: comparison of five molecular fixatives. *J Clin Pathol* **66:** 807–810. doi:10.1136/jclinpath-2012-201283

Sudji IR, Subburaj Y, Frenkel N, García-Sáez AJ, Wink M. 2015. Membrane disintegration caused by the steroid saponin digitonin is related to the presence of cholesterol. *Molecules* **20:** 20146–20160. doi:10.3390/molecules201119682

Sylwestrak EL, Rajasethupathy P, Wright MA, Jaffe A, Deisseroth K. 2016. Multiplexed intact-tissue transcriptional analysis at cellular resolution. *Cell* **164:** 792–804. doi:10.1016/j.cell.2016.01.038

Urieli-Shoval S, Meek RL, Hanson RH, Ferguson M, Gordon D, Benditt EP. 1992. Preservation of RNA for in situ hybridization: Carnoy's versus formaldehyde fixation. *J Histochem Cytochem* **40:** 1879–1885. doi:10.1177/40.12.1280665

Villaseñor R, Nonaka H, Del Conte-Zerial P, Kalaidzidis Y, Zerial M. 2015. Regulation of EGFR signal transduction by analogue-to-digital conversion in endosomes. *Elife* **4:** e06156. doi:10.7554/eLife.06156

Yanez Arteta M, Kjellman T, Bartesaghi S, Wallin S, Wu X, Kvist AJ, Dabkowska A, Székely N, Radulescu A, Bergenholtz J, et al. 2018. Successful reprogramming of cellular protein production through mRNA delivered by functionalized lipid nanoparticles. *Proc Natl Acad Sci* **115:** E3351–E3360. doi:10.1073/pnas.1720542115

Zhigaltsev IV, Belliveau N, Hafez I, Leung AKK, Huft J, Hansen C, Cullis PR. 2012. Bottom-up design and synthesis of limit size lipid nanoparticle systems with aqueous and triglyceride cores using millisecond microfluidic mixing. *Langmuir* **28:** 3633–3640. doi:10.1021/la204833h